Original Paper

Ultrasound versus Cone-beam CT image-guided radiotherapy for prostate and post-prostatectomy pretreatment localization

Marie Fargier-Voiron [a,b,c,d,e,f], Benoît Presles [a,b,c,d,e,f], Pascal Pommier [g], Alexandre Munoz [g], Simon Rit [a,b,c,d,e,f], David Sarrut [a,b,c,d,e,f], Marie-Claude Biston [a,b,c,d,e,f,*]

[a] CREATIS, Université de Lyon, Lyon, France
[b] CNRS UMR5220, Lyon, France
[c] Inserm U1044, Lyon, France
[d] INSA-Lyon, Lyon, France
[e] Université Lyon 1, Lyon, France
[f] Centre Léon Bérard, Lyon, France
[g] Léon Bérard Cancer Center, University of Lyon, F-69373 Lyon, France

ABSTRACT

Purpose: To evaluate the accuracy of an intra-modality trans-abdominal ultrasound (TA-US) device against soft-tissue based Cone-Beam Computed tomography (CBCT) registration for prostate and post-prostatectomy pre-treatment positioning.
Methods: The differences between CBCT and US shifts were calculated on 25 prostate cancer patients (cohort A) and 11 post-prostatectomy patients (cohort B), resulting in 284 and 106 paired shifts for cohorts A and B, respectively. As a second step, a corrective method was applied to the US registration results to decrease the systematic shifts observed between TA-US and CBCT results. This method consisted of sub-tracting the mean difference obtained between US and CBCT registration results during the first 3 sessions from the US registration results of the subsequent sessions. Inter-operator registration variability (IOV) was also investigated for both modalities.
Results: After initial review, about 20% of the US images were excluded because of insufficient quality. The average differences between US and CBCT were: 2.8 ± 4.1 mm, -0.9 ± 4.2 mm, 0.4 ± 3.4 mm for cohort A and 1.3 ± 5.0 mm, -2.3 ± 4.6 mm, 0.5 ± 2.9 mm for cohort B, in the anterior-posterior (AP), superior-inferior (SI) and lateral (LR) directions, respectively. After applying the corrective method, only the differences in the AP direction remained significant ($p < 0.05$). The IOV values were between 0.6–2.0 mm and 2.1–3.5 mm for the CBCT and TA-US modalities, respectively.
Conclusions: Based on the obtained results and on the image quality, the TA-US imaging modality is not safely interchangeable with CBCT for pre-treatment repositioning. Treatment margins adaptation based on the correction of the systematic shifts should be considered.

© 2015 Associazione Italiana di Fisica Medica. Published by Elsevier Ltd. All rights reserved.

Introduction

For accurate dose delivery in prostate cancer radiotherapy, a robust image-guided radiotherapy (IGRT) strategy based on soft tissue registration is required since some studies have shown that movements of prostate and bones are not correlated [1]. Indeed it has been shown that patient positioning with soft-tissue CBCT significantly reduced acute genitourinary toxicity compared to positioning with EPID

without fiducial markers (FM) [2]. Two main categories of soft tissue IGRT modalities can be defined. The first category uses implanted surrogates for target localization, such as FM or implanted electro-magnetic transponders [3,4]. Even though these techniques are relevant for prostate positioning, the associated risks with the surgical implantation of surrogates cannot be neglected, as well as the possibility for them to migrate during the treatment course [5]. Furthermore, the use of FM requires an X-ray imaging modality, such as megavolt electronic portal imaging (MV-EPI) or kilovolt projection imaging. The second category encompasses imaging modalities enabling a 3D acquisition such as CT-on-rails, cone beam computed tomography (CBCT), cine magnetic resonance imaging and ultrasound (US) imaging [6–13]. Among these modalities, CBCT is the most used. It allows a 3D visualization of both target volume

and organs at risk, but involves a non-negligible additional dose to the patient [14]. Therefore, US imaging appears to be an interesting alternative since it is non-invasive and non-irradiating and thus does not imply any associated risk for the patient.

Three transabdominal US systems (TA-US) were commercialized over the past 15 years. The BAT® [12] (Nomos, Pittsburg, USA) and SonArray® [13] (Varian, Palo Alto, USA) devices are based on an inter-modality registration that consists of projecting the CT contours on the US treatment image to determine target misalignments. In contrast, the Clarity device (Elekta, Stockholm, Sweden) is an intra-modality system that compares a daily TA-US image acquired at the beginning of the treatment session to a reference TA-US image acquired during the planning CT acquisition [6–11]. Three studies have reported results on the accuracy of the Clarity TA-US system in clinical conditions. These studies were only performed on prostate patients and not on post-prostatectomy patients [7,9,10]. The system was compared with either MV-EPI associated with FM implants [7,10], or with 2D-kV bony registration and CBCT registration with FM or transponder implants [9]. All studies reported large discrepancies between the different modalities, with percentage of shifts agreement at 5 mm between 67.4% and 85.1%, and larger systematic errors found with the US device. Post-prostatectomy patients positioning comparisons between US imaging and another IGRT modality were investigated in one particular study [15]. They compared the registration results obtained with the inter-modality BAT system and the CT-on-rails device. The use of the US imaging was reported to be beneficial, but only if initial displacements of the prostate bed were larger than 4 mm. For displacements smaller than 4 mm the technique neither improved nor worsened target localization.

The Clarity TA-US device was installed 3 years ago in our department with the objective to replace soft-tissue based CBCT registration for both prostate and post-prostatectomy patients. To our knowledge, this is the first study reporting on the use of the Clarity system for post-prostatectomy positioning. Likewise, prostate positioning comparison between TA-US and a non-invasive volumetric imaging technique, i.e. without implanted markers, has never been performed in clinical conditions.

Therefore, the first objective of this study was to perform a comparison between TA-US registration and soft-tissue based CBCT registration on both prostate and post-prostatectomy patients. The inter-operator variability for the registration process was evaluated for each configuration. Finally, the potential gain of using the TA-US system routinely for patient positioning was studied by calculating the treatment margins adapted to the US modality.

Materials and methods

The US IGRT system

The 3D US–IGRT system (Clarity®) was described in detail elsewhere [10]. Briefly, it is based on a TA-US probe tracked by an infrared camera. For each acquisition, several hundreds of 2D US slices are acquired during a probe sweep and merged into a 3D image. During the planning CT session, a reference US image (US$_{ref}$) is acquired with the same patient set-up as during the CT acquisition. The US$_{ref}$ image is superimposed directly on the CT image through a room calibration process, allowing visualization of the US$_{ref}$ and CT images in the same coordinate system. Note that images are not registered but only superimposed. Thus the patient is supposed to be immobile between the 2 acquisitions. A reference positioning volume (RPV) is then delineated on the US$_{ref}$ image. Over the treatment course, a daily US image (US$_{daily}$) is acquired at the beginning of each session, and manually registered on the US$_{ref}$ image by projecting the RPV volume on the US$_{daily}$ image. The accuracy of the system is checked daily by performing US acquisitions on an

ultrasound phantom aligned on the room lasers, ensuring an uncertainty below 1 mm and 2 mm for the reference and the daily US systems, respectively [16].

Patients

This prospective study was approved by the hospital ethics committee. All included patients signed a letter of consent. 38 patients undergoing a prostate irradiation and 15 patients irradiated after prostatectomy were imaged using the TA-US device between July 2012 and November 2013. Planning target volumes (PTVs) were automatically generated by adding a 3D 7 mm uniform margin around the clinical target volumes for both localizations. The total prescription dose was 66 Gy for post-prostatectomy patients and 74 Gy to the PTV for prostate patients using a standard fractionation (2 Gy per fraction, 5 days a week). For each patient a VMAT plan was generated. The irradiation was delivered using 6-MV photons with an Elekta Synergy machine equipped with a Cone-Beam Computed Tomography (CBCT) device (XVI, Elekta, Stockholm, Sweden). A bladder filling protocol was given to all patients: one hour before the CT acquisition and each treatment session, patients had to empty their bladder and drink 500 mL of water. Special low-fiber diet instructions were also given before the treatment for the rectum preparation.

10 patients treated from July to October 2012 were excluded from this study to allow the radiation therapists (RT) to acquire some experience with the TA-US device. Likewise, 6 other patients were also excluded due to difficulty maintaining an adequate bladder filling during the treatment. Therefore, results were analyzed on 25 prostate patients (cohort A) and 11 post-prostatectomy patients (cohort B).

All patients were scanned in supine position, with 3 mm slice thickness and standard prostate protocol on a Brilliance CT Big Bore scanner (Philips Medical Systems, Best, The Netherlands). They were immobilized using a cushion under the knees. The same position was kept after the CT acquisition to acquire the US$_{ref}$ image. The approximate time between US$_{ref}$ and CT acquisitions was estimated to 3 minutes. For cohort A, the RPV was the whole or easily visible part of the prostate. The delineation was done semi-automatically by firstly contouring 2 or 3 axial and sagittal slices and using an automatic interpolation. If needed, a manual correction was applied. For cohort B, the RPV corresponded to the bladder neck since it was included in the clinical target volume according to the EORTC guidelines [17] (Fig. 1). To delineate this volume, the entire bladder was contoured on the US$_{ref}$ image, then the volume was truncated superiorly, leaving only the bladder neck [18]. This was a fully manual process.

Image and data processing

In this study, US acquisitions were performed for data collection only. The patient repositioning was always carried out based on CBCT/CT registration results.

US acquisitions were performed at the beginning of each treatment session after laser-guided patient alignment. CBCT images were acquired directly after US$_{daily}$ imaging in order to minimize the patient motion. Some patients were included in daily IGRT protocols, and others were imaged according to the "extended No Action Level" (eNAL) protocol [19], which consists of acquiring one CBCT/US$_{daily}$ image during the first 3 irradiation sessions, and one CBCT/US$_{daily}$ image per week until the end of the treatment.

Registration of CBCT images on the reference CT was done semi-automatically. First, an automatic bony alignment was performed using a clip box including pubic bones, using the XVI software. Then, a manual adjustment was done on the soft tissue target volume, i.e. the prostate for prostate patients and the prostatic bed for
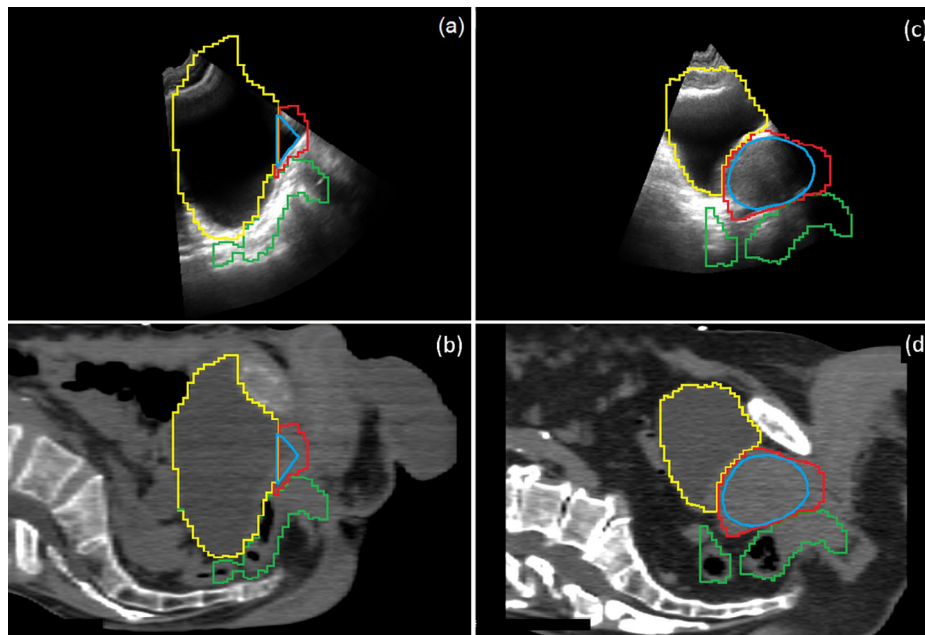
Figure 1. Sagittal slices of post-prostatectomy (a and b) and prostate (c and d) patients of US (a and c) and CT (b and d) acquisitions. Blue, red, yellow and green contours correspond to the RPV, CTV, bladder and rectum volumes, respectively. (For interpretation of the references to color in this figure legend, the reader is referred to the web version of this article.)

post-prostatectomy patients. A total of 337 and 138 paired US and CBCT translational shifts were collected for prostate and post-prostatectomy irradiations, respectively. Rotations were not considered in this study. The required time for US and CBCT acquisitions and registrations processes was measured on different patient sessions. This was estimated to 2 and 5 minutes for US and CBCT modalities, respectively.

The quality of each US_{daily} image was reviewed before any analysis. 16.9% and 22.1% of the US_{daily} images were excluded from the analysis for prostate and post-prostatectomy patients, respectively, mainly because of insufficient bladder filling or 3D reconstruction problems. Ultimately, the analysis concerned 25 patients and 284 paired shifts for cohort A, and 11 patients and 106 paired shifts for cohort B. This data set is denoted *raw database*.

For patient p and session s, the resulting shifts were denoted $T_{CBCT,p,s}$ and $T_{US,p,s}$ for CBCT and US modalities, respectively. For each session, the difference between CBCT and US shifts was calculated as follows: $\delta_{CBCT-US,p,s} = T_{CBCT,p,s} - T_{US,p,s}$. Means and standard deviations of the differences were calculated over all patients. Paired samples t-tests were performed on the US and CBCT shifts to compare the means of the 2 distributions, the null hypothesis being the equality between them. Statistical significance of the outcome was assumed for a p-value below 0.05.

To determine whether CBCT and US imaging had the same accuracy for target localization, the 95% limits of agreement (LOA) were calculated using the Bland–Altman method [20] for each localization and each direction as follows: LOA = b ± 1.96*SD, where b is the bias, i.e. the mean of the differences between CBCT and US measurements, and SD the standard deviation of the differences between CBCT and US measurements. It corresponds to the range within which 95% of differences lie, assuming the differences are normally distributed. This assumption was assessed by plotting the frequency histograms. If the limits are above a predefined tolerance, the 2 modalities cannot be interchanged without causing a relevant difference. Shift agreements at ±5 mm, i.e. the number of sessions for which the difference between the 2 modalities is below 5 mm, were also calculated.

Finally, since CT and US_{ref} images were not acquired simultaneously, systematic differences were expected between the 2 registration modalities. The average of the $\delta_{CBCT-US,p,s}$ values was calculated over the first 3 sessions for each patient as follows: $\Delta_{mean} = (\delta_{CBCT-US,p,1} + \delta_{CBCT-US,p,2} + \delta_{CBCT-US,p,3})/3$. This value was retrospectively applied to the subsequent $T_{US,p,s}$ values to correct for the systematic differences observed between CBCT and US shifts. The statistical analysis described above was repeated on this new data set, denoted *corrected database*.

Treatment margins

Treatment margins assuming a patient alignment based on US registration results were calculated for the raw and corrected databases using the residual shift after US repositioning, i.e. the difference between the US and CBCT shifts. For this calculation, only interfraction uncertainties were taken into account and CBCT registration was used as the reference position.

The interfraction mean error, $\mu_{interfraction}$, the standard deviation of the mean, $\Sigma_{interfraction}$, and the root mean square of the standard deviations, $\sigma_{interfraction}$, were computed based on shifts obtained with each imaging method. In each direction, margins were calculated using the van Herk formula [21] as follows:

$$M = 2.5 * \sqrt{\Sigma_{pressure}^2 + \Sigma_{interfraction}^2} + 0.7 * \sqrt{\sigma_{pressure}^2 + \sigma_{interfraction}^2 + \sigma_{inter-operator}^2}$$

$\Sigma_{pressure}$ and $\sigma_{pressure}$ represent the errors due to the displacement of the prostate induced by different probe pressure levels. These errors were taken from a previous study [22]. $\sigma_{inter-operator}$ represents the error due to the inter-operator registration variability which was calculated as described below.

Inter-operator variability

For a subset of 74 images of 4 patients in cohort A and 62 images of 7 patients in cohort B, CBCT/CT and US_{daily}/US_{ref} registrations were

retrospectively done separately by one expert and 3 well-trained RTs to estimate the inter-operator variability of the registration process of each modality. The standard deviation $\sigma_{p,s}$ for each session s of patient p was calculated over the 4 operators. Inter-operator variability (IOV) was calculated in each direction as follows: $IOV = RMS_p(RMS_s(\sigma_{p,s}))$, with RMS_p and RMS_s being the root mean square over all patients and the root mean square over all sessions of the same patient, respectively.

Results

Target localization using CBCT and US modalities

The differences observed between CBCT and US measurements in target localization, using the raw and corrected databases, ($\delta_{CBCT-US,p,s}$ values) are shown in Figs. 2 and 3 for cohorts A and B, respectively. When considering the 2 raw databases (prostate/post-prostatectomy), the shift agreement at ±5 mm in all directions was reached for only one post-prostatectomy patient (B7: patient 7 in cohort B). The best agreement between CBCT and US registrations was found in the LR direction. The largest discrepancies were ob-
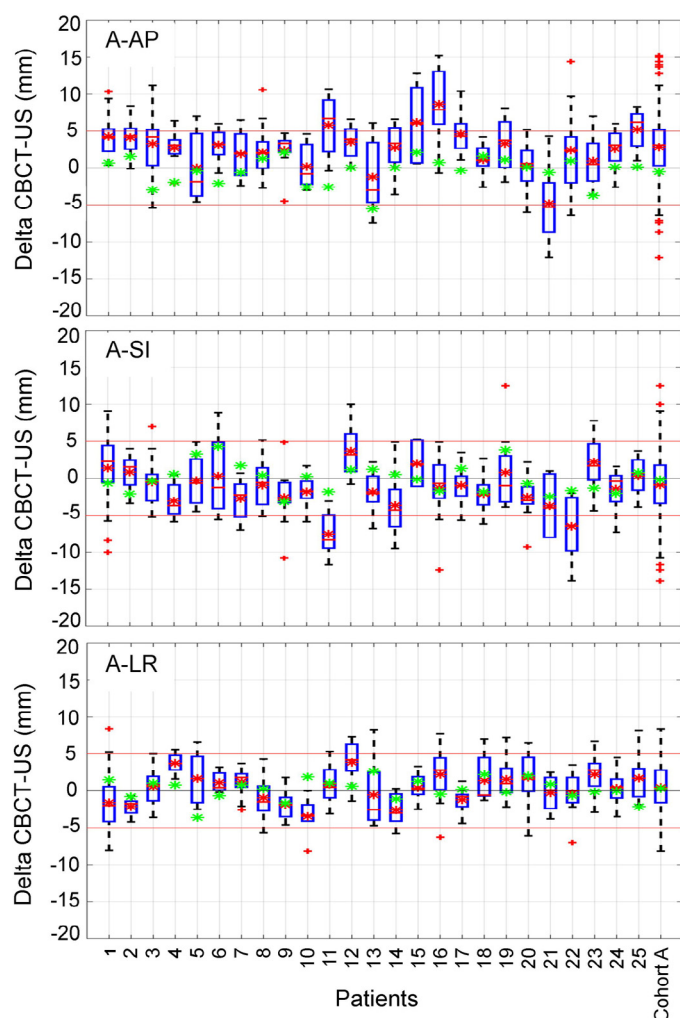
Figure 2. Differences between CBCT and US shifts for patients of cohort A in AP, SI and LR directions. Box-and-whisker plots represent the median of the raw dataset (red dash), the 25th and 75th percentiles (edges of the box), and total range (extent of whiskers). Red and green asterisks represent the mean values of raw and corrected datasets, respectively. The red lines represent the ±5 mm range. (For interpretation of the references to color in this figure legend, the reader is referred to the web version of this article.)
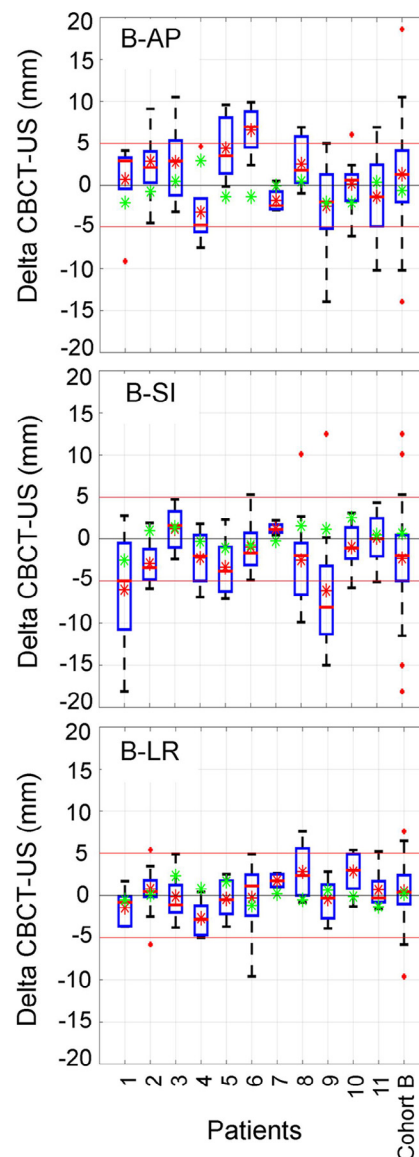
Figure 3. Differences between CBCT and US shifts for patients of cohort B in AP, SI and LR directions. Box-and-whisker plots represent the median of the raw dataset (red dash), the 25th and 75th percentiles (edges of the box), and total range (extent of whiskers). Red and green asterisks represent the mean values of raw and corrected datasets, respectively. The red lines represent the ±5 mm range. (For interpretation of the references to color in this figure legend, the reader is referred to the web version of this article.)

served in the AP direction in cohort A, with higher shifts in the posterior direction for the US compared to the CBCT. For the other axes, the shifts were randomly distributed in the 2 directions. Unlike in cohort A, the most important shifts in cohort B were observed in the inferior direction. These results were confirmed by the statistical data shown in Table 1. The largest systematic difference was found in cohort A in the AP direction (2.8 mm). In cohort B, the largest systematic difference was found in the SI direction (–2.3 mm), but a difference superior to 1 mm was also observed in the AP direction (1.3 mm). Differences were found statistically significant between the 2 modalities in all directions for both localizations, except for the post-prostatectomy cases in the lateral direction. Finally the LOA values were above ±5 mm in all directions, and even reached 11 mm in the SI and/or AP direction for both localizations.

The corrective method enabled the large systematic differences observed in the AP direction to be corrected for patients A11,

Table 1
Analysis of the differences between paired CBCT and US registration results for cohort A and cohort B. Values are calculated on the raw database and on the database corrected by the mean difference between CBCT and US shifts over the first 3 sessions. For each case, mean, standard deviation and the associated p value are calculated. Shift agreements are given for a range of ±5 mm. Limits of agreement (LOA) are calculated according to the Bland–Altman method.

Cohort direction	Raw database					
	A			B		
	AP	SI	LR	AP	SI	LR
Mean ± std (mm)	2.8 ± 4.1	−0.9 ± 4.2	0.5 ± 3.3	1.3 ± 5.0	−2.3 ± 4.6	0.5 ± 2.9
p Value	<0.05	<0.05	<0.05	<0.05	<0.05	0.06
Shifts agreement (%)	70.4	78.5	87.3	71.7	74.5	91.5
LOA (mm)	[−5.3;10.9]	[−9.0;7.3]	[−5.9;6.9]	[−8.4;11.0]	[−11.3;6.7]	[−5.1;6.2]
Cohort direction	Corrected database					
	A			B		
	AP	SI	LR	AP	SI	LR
Mean ± std (mm)	−0.5 ± 3.9	−1.0 ± 4.2	0.3 ± 3.0	−0.7 ± 4.3	1.0 ± 4.6	0.2 ± 2.7
p Value	<0.05	0.45	0.13	0.11	0.10	0.07
Shifts agreement (%)	81.7	84.5	90.5	80.2	86.8	96.2
LOA (mm)	[−8.1; 7.1]	[−7.7; 7.3]	[−5.6; 6.2]	[−9.1; 7.7]	[−7.6; 8.9]	[−5.0; 5.4]

AP: anterior-posterior, SI: superior-inferior, LR: left-right, std: standard deviation, LOA: limits of agreement.

A15, A16, A25 (Fig. 2) and B6 (Fig. 3). Likewise, systematic differences fell below 5 mm for patients A11, A22 (Fig. 2), and patients B1 and B9 in the SI direction (Fig. 3). After correction, the systematic difference between CBCT and US shifts was above 5 mm for only one patient (A13) in the AP direction. This decrease of the systematic difference was confirmed by the results given in Table 1. The means of the differences between CBCT and US registrations were less than or equal to 1 mm in each direction for all patients. With this method, shift agreements at ±5 mm were above 80%. The corrected US and CBCT distributions were not statistically different, except in the AP direction for cohort A.

Treatment margins

Margin values based on a US alignment and calculated with the raw and corrected databases are shown in Table 2. Margins ranged from 7.0 mm to 12.3 mm with the raw database. Maximum values were found in the AP direction for both cohorts. The corrective method enabled the reduction of systematic errors Σ and led to smaller margins with values ranging from 5.6 mm to 9.4 mm. The

largest margin decrease was found in the AP direction for cohort B (3.4 mm).

Inter-operator variability

Table 3 shows the inter-operator variability for both localizations. The IOV values ranged from 0.6 mm to 2.0 mm and from 2.1 to 3.5 mm for the CBCT and US modalities, respectively. A maximum value of 3.5 mm was found in the AP direction for the US modality for post-prostatectomy localization.

Discussion

The aim of this paper was to investigate the performance of an intra-modality IGRT-US system compared to a soft-tissue based CBCT registration on both prostate and post-prostatectomy patients. To our knowledge, only 2 other studies reported post-prostatectomy positioning results obtained with inter-modality US devices [15,23], but the performance of intra-modality US devices had never been investigated for this localization. The main difficulty with

Table 2
Treatment margin values assuming a patient alignment based on the US registration results. Values are calculated based on the raw and corrected database. Residual shifts after US alignment are assumed to be the difference between CBCT and US registration results.

	Cohort A		
	AP (mm)	SI (mm)	LR (mm)
Probe pressure	$\Sigma_{pressure} = \sigma_{pressure} = 1.3$	$\Sigma_{pressure} = \sigma_{pressure} = 1.5$	$\Sigma_{pressure} = \sigma_{pressure} = 0.5$
Inter-operator registration variability	$\sigma_{IO} = 2.1$	$\sigma_{IO} = 2.6$	$\sigma_{IO} = 2.2$
Interfraction localization errors without correction	$\Sigma_{interfraction} = 2.7$	$\Sigma_{interfraction} = 2.6$	$\Sigma_{interfraction} = 1.9$
	$\sigma_{interfraction} = 3.7$	$\sigma_{interfraction} = 3.5$	$\sigma_{interfraction} = 2.8$
Interfraction localization errors with correction	$\Sigma_{interfraction} = 1.9$	$\Sigma_{interfraction} = 2.0$	$\Sigma_{interfraction} = 1.5$
	$\sigma_{interfraction} = 3.7$	$\sigma_{interfraction} = 3.5$	$\sigma_{interfraction} = 2.8$
Margins without correction	10.6	10.7	7.4
Margins with correction	8.9	9.4	6.4
	Cohort B		
	AP (mm)	SI (mm)	LR (mm)
Probe pressure	$\Sigma_{pressure} = \sigma_{pressure} = 1.3$	$\Sigma_{pressure} = \sigma_{pressure} = 1.5$	$\Sigma_{pressure} = \sigma_{pressure} = 0.5$
Inter-operator registration variability	$\sigma_{IO} = 3.5$	$\sigma_{IO} = 2.5$	$\sigma_{IO} = 2.5$
Interfraction localization errors without correction	$\Sigma_{interfraction} = 3.1$	$\Sigma_{interfraction} = 2.5$	$\Sigma_{interfraction} = 1.7$
	$\sigma_{interfraction} = 4.2$	$\sigma_{interfraction} = 4.4$	$\sigma_{interfraction} = 2.6$
Interfraction localization errors with correction	$\Sigma_{interfraction} = 1.5$	$\Sigma_{interfraction} = 1.4$	$\Sigma_{interfraction} = 1.1$
	$\sigma_{interfraction} = 4.2$	$\sigma_{interfraction} = 4.4$	$\sigma_{interfraction} = 2.6$
Margins without correction	12.3	11.0	7.0
Margins with correction	8.9	8.8	5.6

AP: anterior-posterior, SI: superior-inferior, LR: left-right.

Table 3
Inter-operator variability of registration of CT/CBCT and US/US images for prostate and prostatectomy localizations.

	AP (mm)		SI (mm)		LR (mm)	
	Prostate	Post-Prostatectomy	Prostate	Post-Prostatectomy	Prostate	Post-Prostatectomy
CBCT	2.0	1.1	1.8	0.9	1.1	0.6
US	2.1	3.5	2.6	2.5	2.2	2.5

AP: anterior-posterior, SI: superior-inferior, LR: left-right.

post-prostatectomy localization is to validate a suitable RPV that enables the prostate bed to be located correctly in US images. In the present study, comparable shift agreements were obtained using the bladder neck [71.7–91.5%] or the prostate volume [70.4–87.3%] as RPV when comparing TA-US to CBCT registration. However, whereas the systematic shifts were more pronounced in the posterior direction for prostate patients, for post-prostatectomy patients, there was a trend to have larger differences in the SI direction, with more pronounced shifts in the inferior direction. Two assumptions can explain this observation: first, the difficulty to accurately localize the vesico-ureteric anastomosis on CBCT images [24]; second, the RPV is only defined in the inferior direction on US images, and arbitrarily truncated in the superior direction. Thus, US images registration only relies on one boundary instead of 2 for the other directions (Fig. 1). Finally, for prostate patients, the results obtained in the present study were in agreement with those previously reported, with LOA values close to 10 mm in all directions, and larger discrepancies observed in the AP direction [7,9,10].

Several publications have raised concerns about the accuracy of inter-modality US devices [12,13]. Among the suggested reasons are user variability, the impact of probe pressure on prostate localization [22,25], the speed of sound aberration on 3D-US reconstruction [26], and the differences in the prostate delineation between CT and US modalities [27]. Therefore, it was assumed that a technique based on an intra-modality registration would minimize these errors by eliminating the speed of sound aberration, the differences in the contour visualization and minimizing the impact of the probe pressure. Indeed, the prostate is likely to be shifted relative to the planning CT due to probe pressure. The same shift value will be reported on all the US images if the pressure is kept constant between reference and daily acquisition. Under this condition the interfraction shift reported from intramodality US registration can be taken as the prostate shift, assuming that other sources of errors than probe pressure are negligible. Hence, Cury et al. obtained better results with an intra-modality system than with an inter-modality system, compared to CT/CT registration [6]. However, this study was not performed following a clinical workflow, and implied a small number of patients and images.

While referring to the recent results obtained with various imaging devices compared to the US intra-modality device, the sources of uncertainties remain large enough to be considered before any clinical use. For example, it has been shown that the impact of probe pressure is not completely eliminated since the daily applied pressure can vary between sessions [22]. In addition, the variability of the patient anatomy between simulation and treatment (in particular the bladder filling) can affect the image quality and the accuracy of manual registration. In this study, the inter-operator US registration results showed larger uncertainties (superior to 2 mm in all directions) than CBCT registration results for both prostate and post-prostatectomy patients. These results were obtained without taking into account the impact of probe pressure and operator variability on US scans, which is not an issue for the CBCT, and which worsens the inter-operator US registration process [10]. Furthermore, the manual CBCT registration benefited from a first step based on an automatic registration and was perfected by a manual adjustment on soft tissues. Therefore, developing an automatic tool

for the US registration is an interesting prospect that could minimize this variability [18]. The image quality is another drawback of the TA-US modality. Indeed, for prostate patients, 17% of the images were excluded from the analysis due to poor quality. This issue was even more problematic for the post-prostatectomy patients with 22% of the images excluded. Indeed post-prostatectomy patients had more difficulty maintaining an adequate bladder filling. Furthermore, the bladder neck is closer to the pubic bone than the prostate and requires a larger sweep of the probe, which strengthens the requirement that the bladder be full.

For both localizations, systematic differences were observed in some patients between US and CBCT registrations. The calibration process was not involved, since the systematic differences were patient dependent. A first parameter to consider is the impact of probe pressure on the prostate localization. If the pressure were reproducible, the displacement of prostate due to probe pressure would be identical between US_{ref} and US_{daily} images. However, as shown in Fargier-Voiron et al. pressures applied during treatment are random and can generate errors [22]. Another impacting factor could be that CT and US_{ref} images are not acquired exactly at the same time, which permits intrafraction motion between the 2 acquisitions and can generate systematic differences during the superposition process of the US_{ref} and CT_{ref} images [4]. A solution to correct this possible displacement could be to manually register the TA-US image on the CT image but this would involve additional uncertainties due to the operator variability and to the discrepancies between the volumes visualized on the 2 modalities [27]. These errors induced here are systematics since they occur at the simulation step and will be permanently reproduced during all treatment sessions. Similarly, patients can move between TA-US and CBCT acquisitions, which can potentially generate random errors. Hence, patient movements between acquisitions are likely to explain, in part, the observed differences between the 2 modalities. Daily patient repositioning is required to ensure a uniform and homogeneous dose distribution to the target volume [28], but CBCT modality implies additional dose to the patient (about 30 mGy per CBCT) and longer treatment sessions. Therefore, a method for correcting these systematic shifts was proposed in order to replace CBCT by TA-US after a few sessions. It consisted of using the mean difference of the shifts obtained between the 2 modalities over the first treatment sessions, in order to define a new US_{ref} image position. The number of sessions used for calculating the Δ_{mean} value was chosen so as to have a reliable estimation of the systematic difference, while minimizing the number of sessions with the 2 imaging modalities. With this method, the results were improved for both cohorts since US and CBCT distributions were not statistically different after the correction, except in the AP direction for cohort A. However, this method only corrects the systematic difference, not the large variability observed in the US data. Hence, treatment margins were reduced using the corrected database assuming a patient alignment based on US registration results. However, the random errors σ were not affected and margin values remained superior to 5 mm. Note that multiple operators were involved in the US IGRT process and an inter-observer variability in the acquisition process must be accounted for in margin calculations.

Similarly, the uncertainty in the target delineation was not taken into account in this study. It was shown that this error can increase margin values by 2–3.9 mm [29]. By comparison, soft-tissue CBCT residual shifts were quantified with 2D-MV with FM in a previous study [3]. The obtained systematic and random errors were used with the inter-operator variability found in this study, in order to estimate the required soft-tissue CBCT margins. Values were found smaller than US margins and equal to 7.7 mm, 5.0 mm and 2.3 mm in the AP, SI, and LR directions, respectively.

The main difficulty when comparing 2 IGRT modalities is to define which modality can be considered as a reference for pre-treatment positioning. Indeed, marker-based imaging is subject to inaccuracy due to FM migration or deformation of surrounding tissues. Likewise, poor contrast between structures can affect the accuracy of soft tissue CBCT based imaging. Also, previous works compared soft tissue registration using CBCT and FM with MV-EPI [3,30] registration and reported LOAs up to 6 and 9 mm, which are smaller than the values found in the present paper, but still clinically relevant. In the case of the US intra-modality system, the order of magnitude of the measured discrepancies was similar regardless of IGRT devices used for comparison, which suggests that the TA-US modality is not interchangeable with other IGRT systems without taking into account the issues highlighted in this work.

Conclusion

In this study, we demonstrated the feasibility of using an intra-modality US-based repositioning system for both prostate and post-prostatectomy localizations. However, comparison of registration results obtained with the TA-US and the widespread CBCT showed large differences which are difficult to correct. Therefore, the TA-US device cannot replace CBCT for patient repositioning without increasing treatment margins. Furthermore, TA-US cannot be used as a sole IGRT modality because of a high percentage of low quality images.

Conflict of interest

Acknowledgments

References

[1] Nederveen AJ, Dehnad H, Van Der Heide UA, Van Moorselaar RJ, Hofman P, Lagendijk JJ. Comparison of megavoltage position verification for prostate irradiation based on bony anatomy and implanted fiducials. Radiother Oncol 2003;68:81–8. doi:10.1016/S0167-8140(03)00129-4.

[2] Ost P, De Gersem W, De Potter B, Fonteyne V, De Neve W, De Meerleer G. A comparison of the acute toxicity profile between two-dimensional and three-dimensional image-guided radiotherapy for postoperative prostate cancer. Clin Oncol 2011;23(5):344–9. doi:10.1016/j.clon.2011.01.505.

[3] Moseley DJ, White EA, Wiltshire KL, Rosewall T, Sharpe MB, Siewerdsen JH, et al. Comparison of localization performance with implanted fiducial markers and cone-beam computed tomography for on-line image-guided radiotherapy of the prostate. Int J Radiat Oncol Biol Phys 2007;67(3):942–53. doi:10.1016/j.ijrobp.2006.10.039.

[4] Langen KM, Willoughby TR, Meeks SL, Santhanam A, Cunningham A, Levine L, et al. Observations on real-time prostate gland motion using electromagnetic tracking. Int J Radiat Oncol Biol Phys 2008;71(4):1084–90. doi:10.1016/j.ijrobp.2007.11.054.

[5] Delouya G, Carrier J, Béliveau-Nadeau D, Donath D, Taussky D. Migration of intraprostatic fiducial markers and its influence on the matching quality in external beam radiation therapy for prostate cancer. Radiother Oncol 2010;96(1):43–7. doi:10.1016/j.radonc.2010.03.017.

[6] Cury FL, Shenouda G, Souhami L, Duclos M, Faria SL, David M, et al. Ultrasound-based image guided radiotherapy for prostate cancer: comparison of cross-modality and intramodality methods for daily localization during external beam radiotherapy. Int J Radiat Oncol Biol Phys 2006;66(5):1562–7. doi:10.1016/j.ijrobp.2006.07.1375.

[7] Johnston H, Hilts M, Beckham W, Berthelet E. 3D ultrasound for prostate localization in radiation therapy: a comparison with implanted fiducial markers. Med Phys 2008;35(6):2403. doi:10.1118/1.2924208.

[8] Robinson D, Liu D, Steciw S, Field C, Daly H, Saibishkumar EP, et al. An evaluation of the Clarity 3D ultrasound system for prostate localization. J Appl Clin Med Phys 2012;13(4):3753.

[9] Mayyas E, Chetty IJ, Chetvertkov M, Wen N, Neicu T, Nurushev T, et al. Evaluation of multiple image-based modalities for image-guided radiation therapy (IGRT) of prostate carcinoma: a prospective study. Med Phys 2013;40(4):041707. doi:10.1118/1.4794502.

[10] Van der Meer S, Bloemen-van Gurp E, Hermans J, Voncken R, Heuvelmans D, Gubbels C, et al. Critical assessment of intramodality 3D ultrasound imaging for prostate IGRT compared to fiducial markers. Med Phys 2013;40(7):071707. doi:10.1118/1.4808359.

[11] Martyn M, Kleefeld C, Moore M, Foley M. Clinical evaluation of inter-fractional organ motion using 3D ultrasound image-guided radiotherapy for positioning prostate cancer patients. Phys Med 2013;30(6):720. doi:10.1016/j.ejmp.2014.06.018.

[12] Boda-Heggemann J, Köhler FM, Küpper B, Wolff D, Wertz H, Mai S, et al. Accuracy of ultrasound-based (BAT) prostate-repositioning: a three-dimensional on-line fiducial-based assessment with cone-beam computed tomography. Int J Radiat Oncol Biol Phys 2008;70(4):1247–55. doi:10.1016/j.ijrobp.2007.12.003.

[13] Peignaux K, Truc G, Barillot I, Ammor A. Clinical assessment of the use of the Sonarray system for daily prostate localization. Radiother Oncol 2006;81:176–8. doi:10.1016/j.radonc.2006.08.027.

[14] Perks JR, Chen AM, Yang CC, Stern RL, Purdy JA. Comparison of peripheral dose from image-guided radiation therapy (IGRT) using kV cone beam CT to intensity-modulated radiation therapy (IMRT). Radiother Oncol 2009;89:304–10. doi:10.1016/j.radonc.2008.07.026.

[15] Paskalev K, Feigenberg S, Jacob R, McNeeley S, Horwitz E, Price R, et al. Target localization for post-prostatectomy patients using CT and ultrasound image guidance. J Appl Clin Med Phys 2005;6(4):40–9.

[16] Lachaine M, Falco T. Intrafractional prostate motion management with the clarity autoscan system. Med Phys Int 2013;1(1):72–80. <http://federation-fampo.org/web/uploads/MPI-2013-01.pdf#page=72>; [accessed 09.12.14].

[17] Poortmans P, Bossi A, Vandeputte K, Bosset M, Miralbell R, Maingon P, et al. Guidelines for target volume definition in post-operative radiotherapy for prostate cancer, on behalf of the EORTC Radiation Oncology Group. Radiother Oncol 2007;84(2):121–7. doi:10.1016/j.radonc.2007.07.017.

[18] Presles B, Fargier-Voiron M, Biston M. Semiautomatic registration of 3D transabdominal ultrasound images for patient repositioning during postprostatectomy radiotherapy. Med Phys 2014;41:122903. doi:10.1118/1.4901642.

[19] De Boer HCJ, Heijmen BJM. eNAL: an extension of the NAL setup correction protocol for effective use of weekly follow-up measurements. Int J Radiat Oncol Biol Phys 2007;67(5):1586–95. doi:10.1016/j.ijrobp.2006.11.050.

[20] Bland J, Altman D. Statistical methods for assessing agreement between two methods of clinical measurement. Lancet 1986;327(8476):307–10. doi:10.1016/S0140-6736(86)90837-8.

[21] Van Herk M, Remeijer P, Rasch C, Lebesque JV. The probability of correct target dosage: dose-population histograms for deriving treatment margins in radiotherapy. Int J Radiat Oncol Biol Phys 2000;47(4):1121–35.

[22] Fargier-Voiron M, Presles B, Pommier P, Rit S, Munoz A, Liebgott H, et al. Impact of probe pressure variability on prostate localization for ultrasound-based image-guided radiotherapy. Radiother Oncol 2014;111(1):132–7. doi:10.1016/j.radonc.2014.02.008.

[23] Chinnaiyan P, Tomé W, Patel R, Chappell R, Ritter M. 3D-ultrasound guided radiation therapy in the post-prostatectomy setting. Technol Cancer Res Treat 2003;2(5):455–8.

[24] Gill S, Isiah R, Adams R, Dang K, Siva S, Tai KH, et al. Conventional margins not sufficient for post-prostatectomy prostate bed coverage: an analysis of 477 cone-beam computed tomography scans. Radiother Oncol 2014;110(2):235–9. doi:10.1016/j.radonc.2013.12.004.

[25] Artignan X, Smitsmans MHP, Lebesque JV, Jaffray DA, van Herk M, Bartelink H. Online ultrasound image guidance for radiotherapy of prostate cancer: impact of image acquisition on prostate displacement. Int J Radiat Oncol Biol Phys 2004;59(2):595–601. doi:10.1016/j.ijrobp.2004.01.043.

[26] Fontanarosa D, van der Meer S, Verhaegen F. On the significance of density-induced speed of sound variations on US-guided radiotherapy. Med Phys 2012;39(10):6316–23. doi:10.1118/1.4754650.

[27] Smith WL, Lewis C, Bauman G, Rodrigues G, D'Souza D, Ash R, et al. Prostate volume contouring: a 3D analysis of segmentation using 3DTRUS, CT, and MR. Int J Radiat Oncol Biol Phys 2007;67(4):1238–47. doi:10.1016/j.ijrobp.2006.11.027.

[28] Arnaud A, Maingon P, Gauthier M, Naudy S, Dumas JL, Martin E, et al. Image-guided IMRT for localized prostate cancer with daily repositioning: inferring the difference between planned dose and delivered dose distribution. Phys Med 2014;30(6):669–75. doi:10.1016/j.ejmp.2014.04.006.

[29] Rasch C, Steenbakkers R, Van Herk M. Target definition in prostate, head, and neck. Semin Radiat Oncol 2005;15(3):136–45. doi:10.1016/j.semradonc.2005.01.005.

[30] Barney BM, Lee RJ, Handrahan D, Welsh KT, Cook JT, Sause WT. Image-guided radiotherapy (IGRT) for prostate cancer comparing kV imaging of fiducial markers with cone beam computed tomography (CBCT). Int J Radiat Oncol Biol Phys 2011;80(1):301–5. doi:10.1016/j.ijrobp.2010.06.007.